Biomedical Signal Processing and Control 34 (2017) 214–219

Contents lists available at ScienceDirect

Biomedical Signal Processing and Control

journal homepage: www.elsevier.com/locate/bspc

Modulation of spatial variance of ventricular repolarization after myocardial infarction

Maria P. Bonomini[a,b,*], Pedro D. Arini[a,b]

[a] Instituto de Ingeniería Biomédica, Facultad de Ingeniería, Universidad de Buenos Aires, Argentina
[b] Instituto Argentino de Matemática, 'Alberto P. Calderón' CONICET, Buenos Aires, Argentina

ARTICLE INFO

Article history:
Received 9 August 2016
Received in revised form 1 December 2016
Accepted 25 January 2017

Keywords:
Spatial variance
Healing and healed phase
Myocardial infarction
Ventricular fibrillation

ABSTRACT

Background: Myocardial infarction (MI) alters spatial features of the surface electrocardiogram. Spatial variance of the T-wave (SV_T) describes the interlead dispersion about a mean T-wave morphology. SV_T was linked to arrhythmia vulnerability and sudden cardiac death.
Methods: Herein, we studied the evolution of SV_T over the healing (MI_7, up to 7 days after MI) and healed (MI_{60}, from 60 days on post-MI) stages. A control group ($n = 49$) was compared to paired MI_7 and MI_{60} groups ($n = 39$). Five representative sets of frontal and precordial leads were analyzed: $I–II–III$, $V_1 – V_2 – V_3$, $V_4 – V_5 – V_6$, $aV_F – V_2 – V_5$ and $II – aV_F – V_5$.
Results: SV_T index significantly increased at MI_7 ($p < 0.05$) in four out of five sets and returned towards control values at MI_{60} (p = NS). The *preferential combination of ECG leads* resulted $aV_F – V_2 – V_5$, since it showed the strongest modulation. In order to test whether such a modulation was maintained on the presence of ventricular tachycardia and/or ventricular fibrillation (VT/VF), recordings from VT/VF patients were also analyzed. SV_T modulation was lost in the VT/VF group, significantly increasing from controls at MI_{60} ($p < 0.05$) for all sets of leads tested.
Conclusions: SV_T modulation over MI_7 and MI_{60} would signal a good recovery from MI, whereas lack of this modulation could herald a VT/VF event.

1. Introduction

It is well described the cascade of changes in membrane properties that myocardial infarction (MI) induces across the entire heart. More specifically, it can be observed a reduction of peak L-type inward Ca^{2+} in myocites from the epicardial border zone (EBZ) [1] as well as a delayed recovery of the transient inward Na^+ current [2]. Furthermore, myocardium outside the EBZ also presents changes with infarction, such as a prolongation of action potential durations (APDs) during chronic MI [3] or a reduction of transient outward K^+ currents [2]. Besides the changes in ionic currents, proliferation of connective tissue and edema contribute to the nonuniform anisotropy. As a result, it is expected that ECG morphology is altered. More specifically, the interlead morphology differences appearing simultaneously in one beat are expected to change from health to disease. Second central moment analysis, also known as variance, helps quantitate the interlead heterogeneity (or spatial variance) of the entire T-wave morphology recorded from multiple ECG leads. In this regard, many reports focussed on the spatial variance of repolarization in experimental ischemia [4], heart failure [5], MI patients [6] or the general population [7]. Certainly, all these changes are not static, but evolve with time. Pinto and Boyden reviewed the changes in infarcted and non-infarcted cells occurring at different times following MI [8]. During the first week post-MI, so-called healing phase, there exists a shortening and shrinking of action potentials [9], while they shift to prolonged APDs with normal voltages in the healed phase, two months after MI [8]. Moreover, it is during the healing phase that increased heterogeneity of the time course of repolarization in the EBZ is origin of inducible ventricular tachycardia (VT) and ventricular fibrillation (VF) [2].

The hypothesis behind this work, is that these two distinctive stages would modulate the spatial variance of repolarization, which in turn is associated to the cardiac risk that one MI patient is exposed to. This modulation would be reflected on different electrocardiographic markers, such as the T-wave spectral variance, as recently described by Arini and Valverde [10]. Therefore, our

* Corresponding author at: Instituto Argentino de Matemática (IAM) CONICET, Saavedra 15, Buenos Aires, Argentina; Instituto de Ingeniería Biomédica, FIUBA, Buenos Aires, Argentina.
E-mail addresses: paula.bonomini@conicet.gov.ar (M.P. Bonomini), pedro.arini@conicet.gov.ar (P.D. Arini).

http://dx.doi.org/10.1016/j.bspc.2017.01.014
1746-8094/

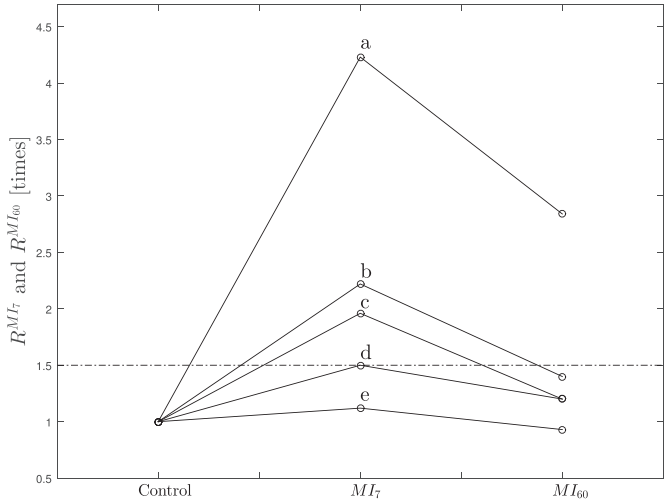

Fig. 1. Relative changes $\mathcal{R}^{MI_7}$ and $\mathcal{R}^{MI_{60}}$ in different sets of leads for control, MI_7 and MI_{60} groups. (a) $V_4 - V_5 - V_6$, (b) $II - aV_F - V_5$, (c) $aV_F - V_2 - V_5$, (d) I–II–III, (e) $V_1 - V_2 - V_3$. Dotted line signals 50% increase with respect to controls. Notice the tendency towards control values at MI_{60} for all the sets.

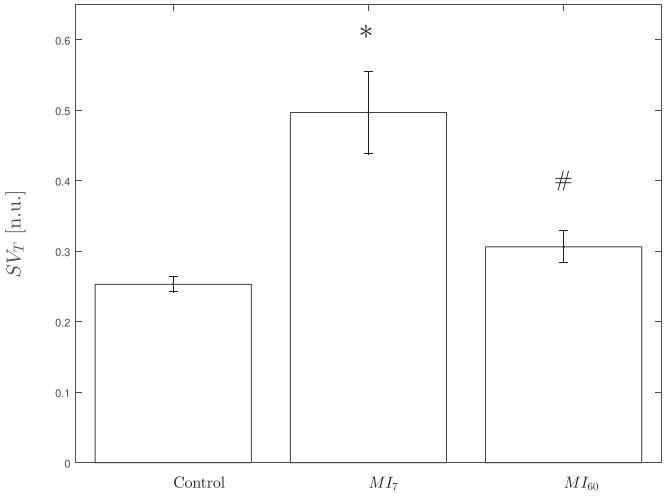

Fig. 2. Mean (SEM) values for SV_T of the *preferential combination of leads* $aV_F - V_2 - V_5$, for control, MI_7 and MI_{60} groups. Notice the tendency towards control values at MI_{60}. *MI_7 vs Control, $p < 0.05$, #MI_7 vs MI_{60}, $p < 0.05$.

main goal is to study the modulation of the spatial variance of the T-wave associated to time elapsed after MI. More specifically, during the healing and healed phases following myocardial infarction. Finally, assess if this modulation is maintained in MI patients showing VT/VF events.

2. Materials and methods

2.1. Database

We have used the Physikalisch-Technische Bundesanstalt (PTB) ECG dataset which is available free on the Physio-Bank [11]. This database comprises 52 healthly subjects and 148 MI patients. The ECGs were digitized at 1000 samples per second, with 16 bit resolution over a range of ±16.384 mV with 2000 A/D units per mV. The recordings are in average 1.35 min long and include 12 standard ECG leads.

We have chosen the following subsets of data, according to the detailed clinical summary included in the PTB dataset [12]: the ECG of healthy subjects (control), $n = 49$ (37 males and 12 females, 43 ± 14 years old), and those infarcted patients without documented ventricular tachycardia (VT) and/or ventricular fibrillation (VF), which simultaneously comprised two ECGs recordings, $n = 39$ (31 males and 8 females, 53 ± 5 years old): one record within the first seven days of MI (MI_7, healing phase), and the other 60 days after MI (MI_{60}, healed phase). In order to asses differences in MI remodeling with occurrence of VT or VF, twenty recordings (ten at MI_7 and ten at MI_{60}) from six patients (3 males and 3 females, 56 ± 2 years old) who underwent such events and presented ECG recordings at both post-MI stages formed the VT/VF counterparts: MI_7^{TF} for the healing phase and MI_{60}^{TF} for the healed phase.

None of the subjects studied had showed bundle branch block or intra-ventricular conduction defects. The QRS durations for healthy subjects were comparable with MI patients. The ECG recordings have been analyzed anonymously, using publicly available secondary data, therefore no ethics statement is required for this investigation [11].

2.2. ECG preprocessing

A set L of five representative combinations of leads were analyzed: $L = \{$I-II-III, $V_1 - V_2 - V_3$, $V_4 - V_5 - V_6$, $aV_F - V_2 - V_5$ and II-$aV_F - V_5\}$. ECG was filtered with a notch filter (Butterworth, 8th order, 50 Hz) to minimize the power-line interference and a cubic spline interpolation filter was used to attenuate ECG baseline drifts and respiratory artifacts [13]. QRS-complexes were detected by means of the wavelet-transform delineator presented in [14]. For every lead $l_i \in L$, a start-up QRS template was built up with the ten first beats and then a new jitter-corrected QRS template was obtained when the cross-correlation coefficient between every new QRS complex and the QRS template was greater than 98%, otherwise the complex was rejected.

2.3. Spatial variance of ventricular repolarization

The spatial variance of the T-wave morphology (SV_T) was calculated using several interlead combinations. These leads were selected from 12 standard ECG leads according to the following criterion: bipolar frontal leads, right and left precordial leads and combinations of frontal and precordial leads. The method to compute spatial variance was modified from Nearing et al. [4], and consists in measuring the splay of waveforms around a mean waveform in a certain set of leads. Briefly, sinusal QRS-complexes were identified and a unique R-wave fiducial point was obtained as the median of the all R-wave marks. Then, for every *jth* beat, a segmentation window W_j^T from 60 to 290 ms after the R-wave occurence was defined, so that the repolarization process was fully covered. After that, T-wave amplitude was normalized and isoelectric level was made uniform for every lead $l_i \in L$, and T-waves of all sinusal beats were superimposed along the ensamble. The T-wave interlead average was accomplished as follows,

$$\bar{T}(n) = \frac{1}{N}\sum_{i=1}^{N} T_i(n) \tag{1}$$

where $T_i(n)$ was the amplitude at sample n $\in W_j^T$, of every jth T-wave in $l_i \in L$, with $N = 3$ leads. After that, the interlead variance was computed along the ensamble as in Eq. (2):

$$\sigma_T(n) = \sqrt{\frac{1}{N}\sum_{i=1}^{N}[T_i(n) - \bar{T}(n)]^2} \tag{2}$$

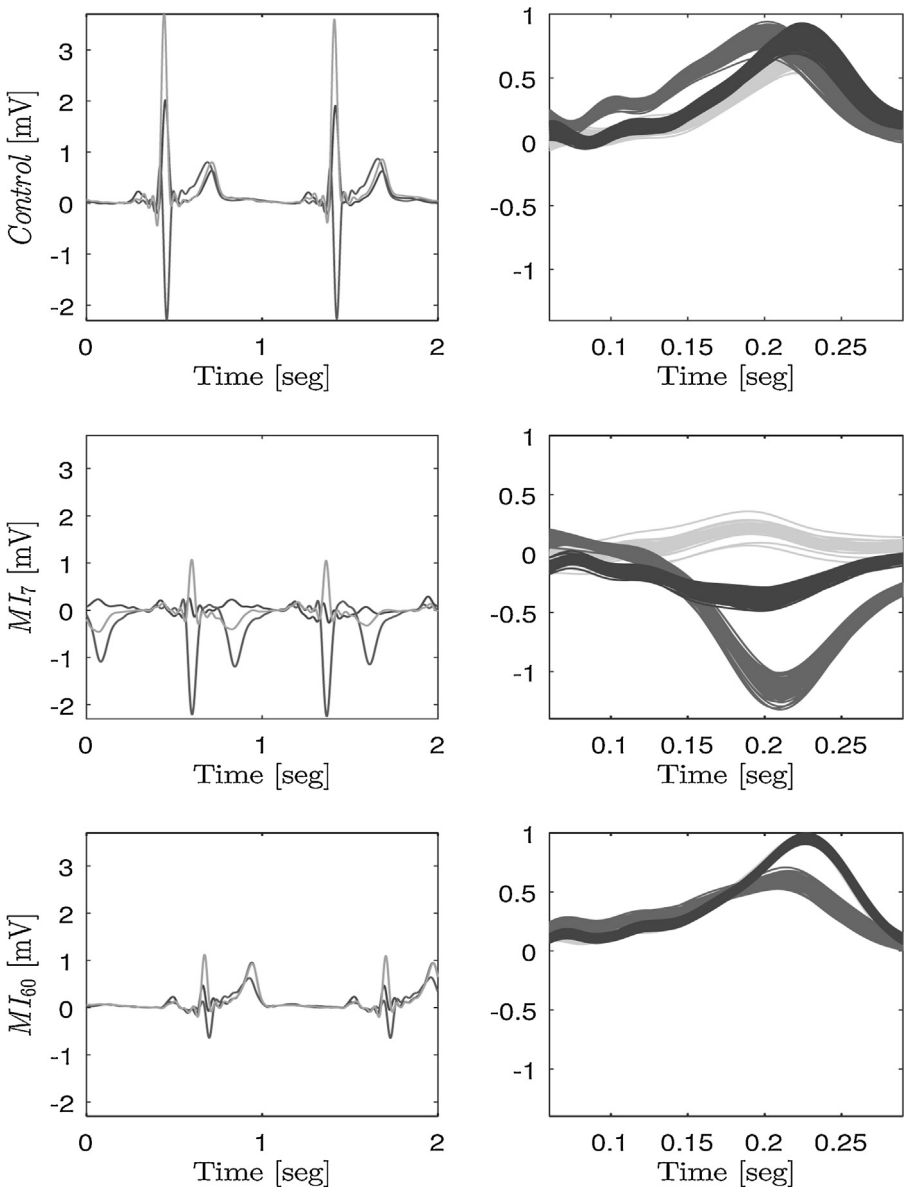

Fig. 3. Representative example of T-wave spatial variance for Control (top), MI_7 and MI_{60} stages for the *preferential combination of leads*. Left: $aV_F - V_2 - V_5$ lead traces. Right: superimposed T-waves on which SV_T was computed. Numbers in left panel show mean SV_T values for that recording.

and the SV_T was then defined as the maximum variance occurring in the analyzed window W_j^T. Thus,

$$SV_T = \max_n [\sigma_T(n)] \tag{3}$$

The mean value $\bar{SV_T}^C$ for each lead combination was obtained for control subjects, and, in the same manner, $\bar{SV_T}^{MI_7}$ and $\bar{SV_T}^{MI_{60}}$ were computed.

Finally, for each set of ECG leads tested, the relative change between MI_7 and control group was defined as

$$\mathcal{R}^{MI_7} = \frac{\bar{SV_T}^{MI_7}}{\bar{SV_T}^C} \tag{4}$$

and likewise,

$$\mathcal{R}^{MI_{60}} = \frac{\bar{SV_T}^{MI_{60}}}{\bar{SV_T}^C} \tag{5}$$

In order to test the strength of modulation with the two post-MI stages, the ratio $\mathcal{R}^{MI_7}/\mathcal{R}^{MI_{60}}$ was evaluated.

2.4. Statistical analysis

With the aim to determine the statistical significance of SV_T index between Control, MI_7 and MI_{60} groups, the SV_T was computed for each patient on every single beat. Moreover, in order to evaluate the influence of the heart rate and the QRS duration in the estimation of SV_T, we analyzed the RR interval and QRS duration along the total beats considered for Control situation, MI_7 and MI_{60}. Mean values of RR intervals and QRS duration for all subsets were computed by averaging the mean RR interval and QRS duration of each subject.

The D'Agostino–Pearson normality test was applied to quantify the discrepancy between the distribution of the parameters and an ideal Gaussian distribution. Since normality was not achieved, the non-parametric two-sided Mann–Whitney *U* test was used for unpaired groups and the Wilcoxon sign rank test for paired data. When p value was <0.05, diferences were considered statistically significant.

3. Results

3.1. SV_T and ECG leads

The SV_T was calculated for every beat on every patient during control, MI_7 and MI_{60} subsets. A non-parametric two-sided Mann–Whitney U test was used between control and MI_7 and also between control and MI_{60}. A Wilcoxon sign rank test was used between MI_7 and MI_{60}. The RR interval, expressed as mean ± SEM, presented statistical significant differences between MI_7 (730 ± 19 ms) and both Control (896 ± 21 ms) and MI_{60} (843 ± 19 ms), $p < 0.0005$ respectively. Also, there was no significant statistical difference between Control and MI_{60}. Moreover, the QRS duration showed non-significant differences between Control (84 ± 1 ms) and both MI_7 (87 ± 2 ms) and MI_{60} (89 ± 2 ms), p = NS respectively. Analogously, there was no significant statistical difference between MI_7 and MI_{60}.

In order to test whether the spatial variance of ventricular repolarization is modulated by the two post-MI stages, the following combination of leads were proposed: frontal differential leads $I–II–III$, right and left precordial leads $V_1 - V_2 - V_3$ and $V_4 - V_5 - V_6$ respectively, and combinations of frontal and horizontal leads, such as, $aV_F - V_2 - V_5$ and $II - aV_F - V_5$. Fig. 1 displays the relative change $\mathcal{R}^{MI_7}$ and $\mathcal{R}^{MI_{60}}$ with respect to controls for the above mentioned set of leads. Dotted line signals 50% increase with respect to controls. The strength of the modulation phenomenon, this is, the ratio $\mathcal{R}^{MI_7}/\mathcal{R}^{MI_{60}}$ was evaluated and shown in Table 1 together with the Mean ± SEM SV_T absolute values and statistical significance for Control, MI_7 and MI_{60} for the above sets of leads.

The *preferential combination of ECG leads* chosen to study the SV_T modulation with the two post-MI stages was $aV_F - V_2 - V_5$, because they showed the maximum ratio $\mathcal{R}^{MI_7}/\mathcal{R}^{MI_{60}}$ (see Fig. 1 and Table 1). The mean ± SEM of the SV_T values for such leads and their statistical significant differences are presented in Fig. 2. Also, a representative MI patient and a control subject were put together in Fig. 3 in order to appreciate the interlead differences for MI_7 and Control and the similarities between MI_{60} and Control.

3.2. SV_T and VT/VF

A total of 20 recordings, (10 at MI_7 and 10 at MI_{60}), all of them belonging to patients with documented VT/VF, were included in the SV_T analysis and compared to the former *"No VT/VF"* groups. In order to test whether modulation in MI_7 and MI_{60} groups was preserved, the equivalent "VT/VF" counterparts were formed; MI_7^{TF} and MI_{60}^{TF} for the healing and the healed phases respectively. Comparison was carried out on the same sets of leads as in Fig. 1. Table 2 shows the Mean ± SEM SV_T absolute values and statistical significance for Control, MI_7 and MI_{60}, together with strength of modulation, $\mathcal{R}^{MI_7}/\mathcal{R}^{MI_{60}}$, and Fig. 4 shows the loss of such a modulation for these sets of leads on the "VT/VF" patients. Indeed, none of the sets differed significantly from MI_7 to MI_{60} (see Table 2). Note that 4 out of 5 sets of leads increased less than 50% with respect to controls at MI_7 (see Fig. 4, dotted line), in opposition to the No VT/VF patients (see Fig. 1). Furthermore, Fig. 5 compares the temporal evolution of the SV_T on $aV_F - V_2 - V_5$, for a "No VT/VF" patient (left) and a "VT/VF" patient (right). Notice how modulation is lost in the latter case, with MI_7^{TF} significantly decreasing from MI_7, $p < 0.05$. In turn, MI_7^{TF} and MI_{60}^{TF} showed no statistical differences between each other, but significantly increased from control, $p < 0.05$.

4. Discussion

Modifications in ventricular repolarization (VR) have been found to play an important role in arrhythmogenesis [15]. In this sense, cardiac electrical instability obtained from the assesment of interlead heterogeneity of T-wave morphology index has been shown in experimental [16,17] and clinical studies [5] to track arrhythmia vulnerability and effective antiarrhythmic therapy [18]. Moreover, it has been demonstrated that after MI, patients have a high incidence of ventricular arrhythmias and sudden cardiac death [19]. Also, persistent modifications in heterogeneity of ventricular repolarization constitutes an important cardiac risk indicator in patients with ischemic heart disease [20]. As far as we know, no one has studied the spatial heterogeneity of the T-wave morphology and its influence after MI infarction. More specifically, during the healing and healed phases following MI, both stages associated to electrical remodeling and the reverse remodeling respectively.

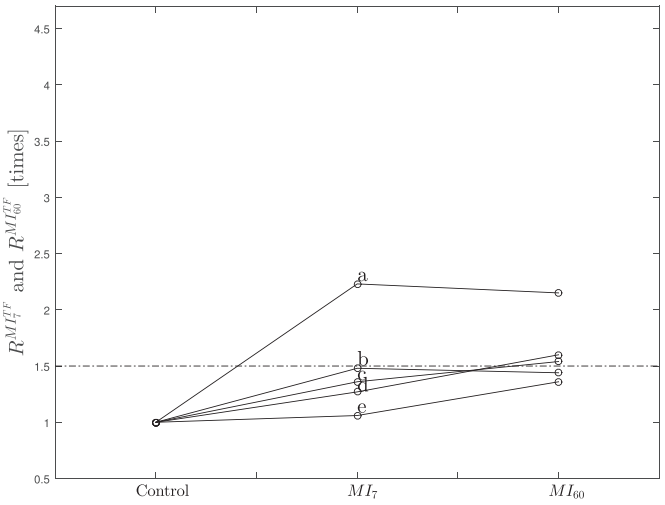

Fig. 4. Relative changes $\mathcal{R}^{MI_7}$ and $\mathcal{R}^{MI_{60}}$ in different set of leads for control, MI_7 and MI_{60} stages on VT/VF patients. (a) $V_4 - V_5 - V_6$, (b) $aV_F - V_2 - V_5$, (c) $II - aV_F - V_5$, (d) $V_1 - V_2 - V_3$, (e) $I–II–III$. Dotted line signals 50% increase with respect to controls. Notice the loss of modulation for all the sets.

4.1. Analysis of SV_T modulation during MI stages

4.1.1. Healing phase in patients without VT/VF

We observed that SV_T at MI_7 was significantly higher from control values for all proposed combinations of leads except for $V_1 - V_2 - V_3$, as can be observed in Table 1. These findings suggest that spatial heterogeneity of VR could be dependent on the combination of ECG leads evaluated. In order to compare quantitatively the strength of the modulation phenomenon among the lead combinations, we computed the ratio $\mathcal{R}^{MI_7}/\mathcal{R}^{MI_{60}}$ for every set, and selected a so-called *preferential combination of ECG leads*, $aV_F - V_2 - V_5$ in this case, reaching maximum differences between MI_7 and MI_{60} (see Table 1).

In general, we consider that the existence of necrotic area in the myocardium could create an increase in the spatial heterogeneity during the healing phase. This assumption relies on two hypothetical ideas. First, the surviving rim of myocites in the epicardial zone of a transmural infarct has been widely studied and termed epicardial border zone (EBZ) [21,9]. The EBZ was proved to elicit VT/VF during the healing phase of MI. It is during this phase that membrane properties in cells of the EBZ are dramatically altered, hence the name of electrical remodeling. There is also presence of edema and proliferation of connective tissue, resulting in nonuniform anisotropy [3]. All these changes could affect the excitability and refractoriness in this zone producing reentry pathways and conduction blocks, leading to an increased cardiac risk. Second, there is evidence that autonomic stimulation modulates the electrical characteristics of the cardiac cells [9]. Besides, transmural MI could disrupt sympathetic and vagal innervation at infarcted sites

Table 1
Mean ± SEM absolute SV_T values and $\mathcal{R}^{MI_7}/\mathcal{R}^{MI_{60}}$ for Control, MI_7 and MI_{60} on the above analyzed sets of leads.

	Controls	MI_7	MI_{60}	$\mathcal{R}^{MI_7}/\mathcal{R}^{MI_{60}}$
I–II–III	0.30 ± 0.011	0.45 ± 0.036**	0.36 ± 0.024†	1.25
$V_1 - V_2 - V_3$	0.33 ± 0.018	0.37 ± 0.048	0.31 ± 0.038	1.20
$V_4 - V_5 - V_6$	0.13 ± 0.007	0.55 ± 0.112***	0.37 ± 0.072#,†	1.48
$aV_F - V_2 - V_5$	0.25 ± 0.010	0.49 ± 0.057***	0.30 ± 0.022†	1.63
II-$aV_F - V_5$	0.22 ± 0.010	0.49 ± 0.060**	0.31 ± 0.033†	1.58

** MI_7 vs Control, $p < 0.005$.
*** MI_7 vs Control, $p < 0.00005$.
# MI_{60} vs Control, $p < 0.005$.
† MI_{60} vs MI_7, $p < 0.005$.

Table 2
Mean ± SEM absolute SV_T values and $\mathcal{R}^{MI_7}/\mathcal{R}^{MI_{60}}$ for Control, MI_7 and MI_{60} on the above analyzed sets of leads on VT/VF patients.

	Controls	MI_7	MI_{60}	$\mathcal{R}^{MI_7}/\mathcal{R}^{MI_{60}}$
I–II–III	0.30 ± 0.011	0.32 ± 0.025	0.41 ± 0.020#	0.78
$V_1 - V_2 - V_3$	0.33 ± 0.018	0.42 ± 0.041	0.53 ± 0.065	0.79
$V_4 - V_5 - V_6$	0.13 ± 0.007	0.29 ± 0.017***	0.28 ± 0.038#	1.03
$aV_F - V_2 - V_5$	0.25 ± 0.010	0.37 ± 0.024***	0.36 ± 0.020#	1.02
II-$aV_F - V_5$	0.20 ± 0.010	0.22 ± 0.016	0.30 ± 0.012#	0.73

*** MI_7 vs Control, $p < 0.00005$.
# MI_{60} vs Control, $p < 0.005$.

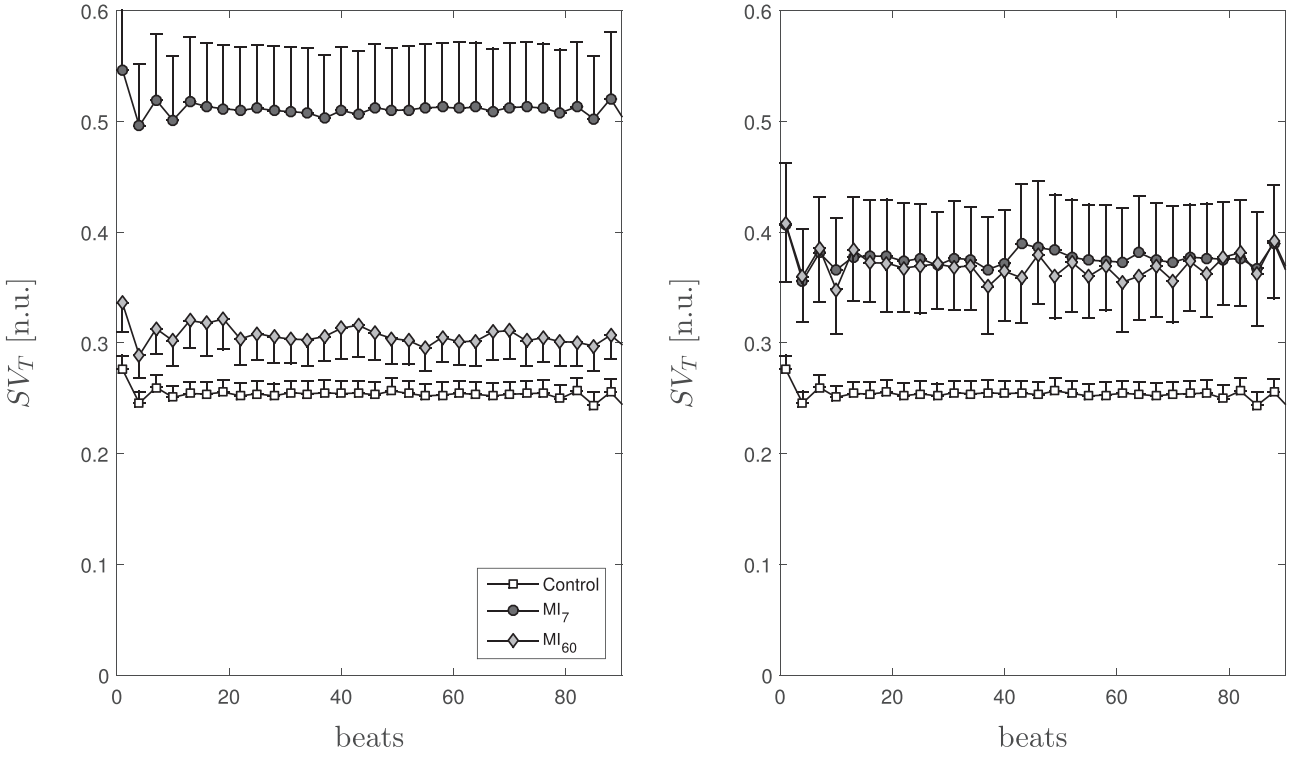

Fig. 5. Temporal evolution of Mean(SEM) SV_T in leads $aV_F - V_2 - V_5$, for control, MI_7 and MI_{60} for patients without VT/VF (left) and with VT/VF (right). Notice the tendency towards control values at MI_{60} for the latter and the distance from controls for the former. *MI_7 vs MI_7^{TF}, $p < 0.05$.

and could produce symphathetic and vagal denervations at noninfarcted zones distal to the necrotic area. These denervated areas of healthy tissue could produce APDs with differential characteristics in comparison to those areas which are normally innervated. This effect produces spatial heterogeneity of repolarization that may be reflected an increase of SV_T index.

4.1.2. Healed phase in patients without VT/VF

It is noted that SV_T at MI_{60} failed to produce significant differences when compared against control SV_T values for any combination of leads analyzed except for $V_1 - V_2 - V_3$ (see Table 1). These results denote that after 60 days of MI, the SV_T indexes for the majority "combinations of ECG leads" tend to decrease toward the control situation. Specially in the *preferential combination of ECG leads* where the modulation strength has the maximum value (see Table 1). The explanation of this phenomenon could be supported by the works of Ursell et al. [9] and Wong et al. [22]. Ursell et al. compared different MI stages, such as: 1–2 weeks post MI (healing stage) and 2–16 months post MI (healed stage) phases of MI. They showed that during the healed phase the APD profiles returned to almost normal values, suggesting the presence of a process that has been denominated "reverse remodeling". Results presented

in [9] were consistent with another previous investigation, based on an animal model, during healed MI phase [22]. We can highlight that surviving endocardial cells have presented characteristics different from those studied during acute ischemia and early infarction, which have prolonged APDs with normal resting membrane potentials and upstroke velocitities [22]. In this context, our results support the hypothesis that, in healed phase of MI there exists a decrement of APD differences, phenomenon that could be translated to a decrease of the SV_T index. That is, the so-called "reverse remodeling", via normalization of the acute changes occurred after MI, would be responsible for the recovery of the spatial heterogeneity of VR, showing values close to those observed in healthy subjects. The "normalization" effects of the reverse remodeling in a population without VT/VF was also evident in the temporal heterogeneity of VR analysis, presented by Arini and Valverde [10], who also found a positive modulation over the healing and healed phases for the T-wave spectral variance, which is strongly associated to T-wave alternans (TWA) and other patterns of periodicity. This analogy makes our very consistent results, since SV_T is clearly linked to TWA [4,5]. Indeed, the rationale for studying the spatial dispersion of interlead morphologies was the appearance of TWA patterns before an ischaemia-induced-ventricular fibrillation in a LAD occlusion model in pigs [4].

4.2. Comparison of SV_T index between patients with and without VT/VF

We have observed, in patients without VT/VF, an increase of the SV_T index during the healing stage, followed by a decrease of the SV_T index at the healed stage (as we showed in Figs. 1 and 2 and Table 1). That is to say, the time elapsed after MI modulated the spatial heterogeneity of the ventricular repolarization, phenomenon quantified by the SV_T index. Conversely, this modulation was lost in patients with VT/VF since SV_T increased further at MI_{60} in most of the sets of leads proposed (see Fig. 4). In particular, SV_T in the *preferential combination of ECG leads* remained 48% above SV_T control values. These results supports those obtained by Nearing et al., where mean T-wave interlead heterogeneity values in a VT population were elevated 52% with respect to those patients without ventricular tachycardia [5].

Moreover, the observation of an increased spatial variance of VR, sustained high, in turn, at MI_{60} in the VT/VF patients is consistent with Kentta et al. [18], who found elevated T-wave interlead heterogeneity in subjects dying from sudden cardiac death in a 7-year followup study from a general population survey. Also, other work, in which the spatial variance of VR was computed over columns and rows of body surface mapping rather than 12-lead ECG, showed an increased spatial variance of repolarization after MI [6], although no information about time elapsed after MI was provided.

5. Conclusions

We have investigated the influence of the time elapsed after myocardial infarction, in particular the healing and healed phases, on spatial variance of ventricular repolarization. Every set of ECG leads analyzed appeared modulated along the two post-MI stages, resulting $aV_F - V_2 - V_5$ the preferential combination, since it showed the strongest modulation in patients without VT/VF events. Finally, we found a differential behavior in the modulation of the SV_T index during healing and healed stages, depending on whether have existed prior VT/VF events.

Acknowledgements

Acknowledgements This work was supported by the Consejo Nacional de Investigaciones Científicas y Técnicas, under Project PIP-538 CONICET, Argentina.

References

[1] R. Aggarwal, J. Pu, P.A. Boyden, Ca(2+)-dependent outward currents in myocytes from epicardial border zone of 5-day infarcted canine heart, Am. J. Physiol. Heart C 273 (3) (1997) H1386–H1394.
[2] F. Aimond, J.L. Alvarez, J.-M. Rauzier, P. Lorente, G. Vassort, Ionic basis of ventricular arrhythmias in remodeled rat heart during long-term myocardial infarction, Cardiovasc. Res. 42 (2) (1999) 402–415.
[3] D. Qin, Z.H. Zhang, E.B. Caref, Cellular and ionic basis of arrhythmias in postinfarction remodeled ventricular myocardium, Circ. Res. 79 (3) (1996) 461–473.
[4] B.D. Nearing, R.L. Verrier, Tracking cardiac electrical instability by computing interlead heterogeneity of T-wave morphology, J. Appl. Physiol. 95 (6) (2003) 2265–2272.
[5] B.D. Nearing, G.A. Wellenius, M.A. Mittleman, M.E. Josephson, A.J. Burger, R.L. Verrier, Crescendo in depolarization and repolarization heterogeneity heralds development of ventricular tachycardia in hospitalized patients with decompensated heart failure, Circ. Arrhythm. Electrophysiol. 5 (1) (2012) 84–90.
[6] B. Khaddoumi, H. Rix, O. Meste, M. Fereniec, R. Maniewski, Body surface ECG signal shape dispersion, IEEE Trans. Biomed. Eng. 53 (12) (2006) 2491–2500.
[7] R.L. Verrier, B.D. Nearing, M.T.L. Rovere, G.D. Pinna, M.A. Mittleman, J.T. Bigger, P.J. Schwartz, A. Investigators, Ambulatory electrocardiogram-based tracking of T wave alternans in postmyocardial infarction patients to assess risk of cardiac arrest or arrhythmic death, J. Cardiovasc. Electrophysiol. 14 (7) (2003) 705–711.
[8] J. Pinto, A. Penelope, P. Boyden, Electrical remodeling in ischemia and infarction, Cardiovasc. Res. 42 (1999) 284–297.
[9] P. Ursell, P. Gardner, A. Albala, J. Fenoglio, A. Wit, Structural and electrophysiological changes in the epicardial border zone of canine myocardial infarcts during infarct healing, Circ. Res. 56 (1985) 436–451.
[10] P. Arini, E. Valverde, Beat-to-beat electrocardiographic analysis of ventricular repolarization variability in patients after myocardial infarction, J. Electrocardiol. 49 (2) (2016) 206–213.
[11] A. Goldberger, L. Amaral, L. Glass, J. Hausdorff, P.H. Ivanov, R. Mark, J. Mietus, G. Moody, C. Peng, H. Stanley, Physiobank, physiotoolkit and physionet: components of a new research resource for complex physiologic signals, Circulation 101 (23) (2000) e215–e220.
[12] R. Bousseljot, D. Kreiseler, A. Schnabel, Nutzung der ekg-signal datenbank cardiodat der PTB über das internet, Biomed. Tech. 40 (1) (1995) 317.
[13] C.R. Meyer, H. Keiser, Electrocardiogram baseline noise estimation and removal using cubic spline and state-space computation techniques, Comput. Biomed. Res. 10 (1977) 459–470.
[14] J.P. Martínez, R. Almeida, S. Olmos, A.P. Rocha, P. Laguna, A wavelet-based ECG delineator: evaluation on standard databases, IEEE Trans. Biomed. Eng. 51 (4) (2004) 570–581.
[15] B. Surawicz, Ventricular fibrillation and dispersion of repolarization, J. Cardiovasc. Electrophysiol. 8 (1997) 1009–1012.
[16] S. Zaho, L.M. Lee, B.D. Nearing, V.O. Busso, K.F. Kwaku, R.L. Verrier, Suppression of calcium-induced repolarization heterogeneity as a mechanism of nitroglycerin's antiarrhythmic action, J. Cardiovasc. Pharmacol. 48 (2006) 22–29.
[17] R.L. Verrier, V.P. Pagotto, A.F. Kanas, M.F. Sobrado, B.D. Nearing, D. Zeng, L. Belardinelli, Low doses of ranolazine and dronedarone in combination exert potent protection against atrial fibrillation and vulnerability to ventricular arrhythmias during acute myocardial ischemia, Heart Rhythm 10 (2013) 121–127.
[18] R. Bonatti, A. Silva, J. Batatinha, L. Sobrado, A. Machado, B. Varone, B. Nearing, L. Belardinelli, R. Verrier, Selective late sodium current blockade with GS-458967 markedly reduces ischemia-induced atrial and ventricular repolarization alternans and ECG heterogeneity, Heart Rhythm 11 (2014) 1827–1835.
[19] J. Myerburg, A. Castellanos, Sudden cardiac death, in: Cardiac Electrophysiology: From Cell to Bedside, Philadelphia, Saunders, Elsevier, 2009.
[20] P.J. Schwartz, S. Wolf, QT interval prolongation as predictor of sudden death in patients with myocardial infarction, Circulation 57 (1978) 1074–1077.
[21] A. Wit, M. Janse, The Ventricular Arrhythmias of Ischemia and Infarction: Electrophysiological Mechanisms, Futura Publishing Company, Mount Kisco, NY, 1993.
[22] S. Wong, A. Basset, J. Cameron, K. Epstein, P. Kozlvskis, R. Myerburg, Dissimilarities in the electrophysiological abnormalities of lateral border and central infarct zone cells after healing of myocardial infarction in cats, Circ. Res. 51 (1982) 486–493.